Advances in Environmental Technology 2 (2021) 119-136

Iranian Reasearch Organization for Science and Technology (IROST)

Advances in Environmental Technology

Journal home page: https://aet.irost.ir/

Response surface methodology approach for simultaneous carbon, nitrogen, and phosphorus removal from industrial wastewater in a sequencing batch reactor

Fatemeh Najartabar Bisheh [a], Malihe Amini[b*], Hajar Abyar[c*], Nicole K. Attenborough[d], Irene Ling [e], Babak Salamatinia[d], Habibollah Younesi[f*], Ali Akbar Zinatizadeh[g]

[a]*Department of Biology, Islamic Azad University, Tonekabon Branch, Tonekabon, Mazandaran, Iran*

[b]*Department of Environmental Science, University of Jiroft, Jiroft, Iran*

[c]*Department of Environmental Sciences, Gorgan University of Agricultural Sciences and Natural Resources, Gorgan, Iran*

[d]*Discipline of Chemical Engineering, School of Engineering, Monash University Malaysia, Jalan Lagoon Selatan, Bandar Sunway, 47500 Subang Jaya, Selangor Malaysia*

[e]*School of Science, Monash University Malaysia, Jalan Lagoon Selatan, Bandar Sunway, 47500 Subang Jaya, Selangor Malaysia*

[f]*Department of Environmental Science, Tarbiat Modares University, Noor, Iran*

[g]*Water and Wastewater Research Center (WWRC), Razi University, Kermanshah, Iran*

ARTICLE INFO

Article history:
Received 22 July 2021
Received in revised form
14 November 2021
Accepted 20 November 2021

Keywords:
Wastewater treatment
Response surface methodology
Granular sludge
SDNR

ABSTRACT

Wastewater reclamation involving a sequencing batch reactor (SBR) has received more attention recently due to its high nutrient removal efficiency, cost-effectiveness, and low footprint. This study attempts to develop a stable and applicable activated sludge SBR for simultaneous carbon and nutrient removal from industrial wastewater. The derived-filed data were explored by response surface methodology (RSM) to identify the impact of operational variables on the SBR performance. Optimum conditions were obtained at 4000 mg/L MLSS, 100: 8: 2 COD: N: P ratio, 40 min/h aeration time, and 40 h cycling time, which resulted in the removal of 82.53% chemical oxygen demand (COD), 89.83% TKN, 87.23% PO_4^{3-}-P, and 73.46% NO_3^--N. Moreover, the sludge volume index (SVI) and mixed liquor volatile suspended solids (MLVSS)/mixed liquor suspended solids (MLSS) ratio were 64.8 mL/g and 0.8, respectively. The maximum nitrification rate was calculated as 113.9 mg/L.d, which increased with the rise of the initial ammonium concentration. The specific denitrification rate (SDNR) was estimated in the range of 0.003-0.07 mgNO_3^-

*Corresponding authors:
Email address: amini.malihe @ujiroft.ac.ir
hajar.abyar@yahoo.com; hunesi@modares.ac.ir
DOI: 10.22104/AET.2021.5093.1383

-N/mg MLVSS.d, depicting the high potential of the SBR reactor to eliminate nitrate by granular sludge. Accordingly, the removal efficiency of the optimized system revealed a notable capability towards meeting environmental regulations.

1. Introduction

Industrial wastewater treatment requires more effective remediation schemes than conventional municipal wastewater treatment systems. Industrial wastewaters are distinctively different in terms of the manufacturing process and their capacity to contaminate water bodies with toxic pollutants. Nutrients such as nitrogen and phosphorus are the significant elements in effluents that threaten aquatic organisms and human beings [1,2]. Moreover, untreated wastewaters containing nutrients provide the opportunity for excessive algal growth leading to oxygen depletion, water quality reduction, unpleasant odor, and eutrophication [3]. Furthermore, high nitrate concentrations in wastewaters can form carcinogenic substances, such as nitrosamines and nitrosamides, and should receive more attention to decrease their harmful concentrations [4]. Conventional technologies such as chemical flocculation, ozonation, polymeric membranes, and adsorption may be efficient and practical for removing dye and other pollutants in wastewaters. But these processes have not been suggested for the treatment of high-strength wastewater due to their low absorbent capacity, secondary pollution, and high cost [5-8]. As a comparison, biological treatment methods are less expensive and more effective, especially for the removal of nitrogen, phosphorus, and carbonaceous substances [9]. Biological nitrogen removal consists of two steps: nitrification and denitrification. Ammonia is converted into nitrite and subsequently into nitrate under the aerobic state in the nitrification process, which is followed by denitrification where nitrite or nitrate is converted into gaseous nitrogen under an anoxic condition [10]. The simultaneous nitrification and denitrification (SND) process is an emerging method for nitrogen removal, which not only saves on the cost of a second anoxic tank and uses more simplified technology [11]. The application of granular sludge in biological wastewater treatment has recently been suggested [12-14]. The microbial aggregates of different bacterial species in large, more compact, and dense granules facilitate the removal process. Their unique features, including high settling velocities and biomass retention, high activity, and ability to resist the high loading rates, have been widely reported in the literature [15,16]. The sequencing batch reactor (SBR) under alternating aerobic/anaerobic conditions seeded with flocculating sludge is appropriate for the formation of granules because of its less rigid operation, low operating costs, and high removal of nitrogen and phosphorus [15]. Although numerous studies have mentioned the outstanding potential of the SBRs for carbon, nitrogen, and phosphorus (CNP) removal, the present study succeeded in not only performing the remarkable simultaneous CNP removal but also improving the nitrification and denitrification rates. RSM could be the best choice to model and optimize the wastewater treatment process in the SBRs. Central composite design (CCD), as an optimization tool of RSM, is useful for building a quadratic model for the response variable. It conveniently reduces the need for repetitive experimentation, notably in designing experiments; on the other hand, it evaluates the interaction of factors affecting the treatment efficiency and provides the optimal condition [17,18]. However, the main objectives of the current investigation were (1) evaluation of SBR performance for COD and nutrient removal from industrial wastewater using RSM; (2) appraisal of interactive effects of four independent variables, namely mixed liquor suspended solids (MLSS) (mg/L), chemical oxygen demand: nitrogen: phosphorus (COD: N: P) ratio, aeration time (min/h), and cycling time (h), and six dependent variables, i.e., removals of COD, total Kjeldahl nitrogen (TKN), PO_4^{3-}, and NO_3^-, sludge volume index (SVI), and mixed liquor volatile suspended solids (MLVSS)/ mixed liquor suspended solids (MLSS) ratio; and (3) quantification of nitrification and denitrification rates.

2. Materials and methods

2.1. Wastewater characterization and seeding sludge

Raw industrial wastewater was retrieved from an equalization tank in an industrial wastewater treatment plant in Amol, Iran. Table 1 summarizes the characteristics of the industrial wastewater. The activated sludge (MLSS of 15000-30000 mg/L), as inoculum, was obtained from the same industrial wastewater.

Table 1. Characteristics of industrial wastewater.

Component	Range (mg/L)	Average ± SD (mg/L)
pH	6.35-7.2	6.79 ± 0.30
TS*	2670-3150	2908 ± 192.61
TSS	250-642	424.44 ± 125.89
VSS	160-402	257.33 ± 58.63
TCOD	1683-2500	2120.72 ± 339.54
SCOD	1140-1670	1419.11 ± 173.32
TBOD	1120-1740	1481.56 ± 249.21
TKN	1.9-13.3	4.75 ± 3.61
NO_3^--N	1.6-9.1	3.79 ± 2.67
PO_4^{3-}-P	5.61-15.345	8.82 ± 2.79

*Total solids (TS), total suspended solids (TSS), volatile suspended solids (VSS), total COD, and soluble COD.

2.2. Experimental design and mathematical model

Design-Expert software (Stat-Ease Inc., version 7.0) and CCD were employed to determine the experimental runs and optimum conditions. Four independent variables (A: MLSS, B: COD: N: P ratio, C: aeration time, and D: cycling time) were selected within the experimental design. The variables in coded and actual units are shown in Table 2 with their corresponding range and level. The experimental design consists of 2^k factorial points accompanied by 2k axial points and a center point with six replications [9]. Consequently, 30 experiments (= $2^k + 2k + 6$) were conducted in this case, where k is the number of factors. Moreover, removals of COD, TKN, PO_4^{3-}, and NO_3^-, as well as the amounts of SVI and MLVSS/MLSS ratio, were considered as responses. Eq.1 represents the empirical second-order polynomial model:

$$Y = \beta_0 + \sum_{i=1}^{k} \beta_i x_i + \sum_{i=1}^{k} \beta_{ii} x_i^2 + \sum_{i=1}^{k-1} \sum_{j=2}^{k} \beta_{ij} x_i x_j + \varepsilon \qquad (1)$$

Where Y is the predicted response and x_i, x_j,..., x_k represent the input variables. In addition, x_i^2; x_j^2;...; x_k^2 are the square effects of the parameters, while $x_i x_j$, $x_i x_k$, and $x_j x_k$ denote the interactional effects of the variables. β_0 shows the intercept, whereby β_i (i = 1,2. . . , k), β_{ii} (i = 1,2. . . , k), and β_{ij} (i = 1,2. . .,k; j = 1,2. . . ,k) symbolize the linear effect, square effect, and the interaction effects, respectively. Also, ε denotes the random error in the system. The *p-value* with a 95% confidence level was considered to evaluate the effectiveness of the model terms. The analysis of variance (ANOVA) was used to show the differences among the studied variables and their impact on the responses.

Table 2. Experimental ranges of the independent variables.

Variables	Range and level				
	-α	-1	0	+1	+ α
A: MLSS, mg/L	1000	2000	3000	4000	5000
B: COD:N:P	100/2/0.5	100/4/1	100/6/1.5	100/8/2	100/10/2.5
C: Aeration time, min/h	35	40	45	50	55
D: Cycling time, h	12	36	60	84	108

2.3. Operation of bioreactor

The lab-scale SBR was fed with 1 L industrial wastewater (Figure 1). Aerated activated sludge was transferred to the system according to the experimental design with concentrations that varied between 1000 mg/L to 5000 mg/L. Furthermore, the activated sludge was aerated by an air diffuser embedded at the bottom of the bioreactor. The NH_4^+ and PO_4^{3-} concentrations were adjusted less than the required amount based on the design parameters (Table 2). Therefore, the essential quantities of nutrients were added to the system to provide an appropriate condition for the activated sludge microorganisms. On the other hand, the programmable timer was utilized to control the operating condition automatically. The industrial wastewater was treated sequentially in aerobic and anaerobic conditions in 12-108 h cycles, including 35–55 min/h for the aeration and 5-25 min/h for an anoxic state, in which the sludge gradually settled. The parameter variations were monitored before and after each experimental run. In addition, the excess sludge was removed from

the system to provide a constant concentration of biomass. The SBR reactor was operated at ambient temperature (25°C ± 2), and the pH of the wastewater was adjusted at 7.

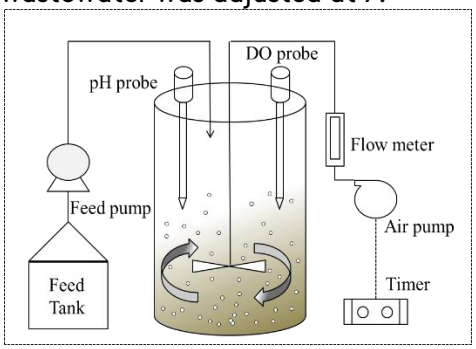

Fig. 1. Sequencing batch reactor.

2.4. Analytical methods

The amounts of COD, TKN, MLSS, MLVSS, SVI, PO_4^{3-}, and NO_3^- were detected by the standard methods [19]. The colorimetric closed reflux coupled with the thermo-reactor system (Aqualytic, AL32, and Germany) was conducted for the COD measurement. The absorbance of COD samples was measured using a spectrophotometer (Aqualytic, Pcespectro, Germany) at a wavelength of 600 nm. The PO_4^{3-} and NO_3^- concentrations were analyzed at a wavelength of 210 and 340 nm, respectively, by a UV-spectrophotometer. The SVI was monitored to show the settling capability of the activated sludge. The pH was measured by a digital, portable pH meter (Hach, HQ40d, Germany).

3. Results and discussion

3.1. Analysis of variance (ANOVA)

The results of the experimental runs are presented in Table 3. Also, Table 4 shows the ANOVA results for all responses and the four variables in coded values. The model significance was determined according to the *p-value,* which was less than 0.0001 for all the dependent variables, indicating the significant relationship between the model and the actual data. The coefficient of determination (R^2) for the dependent variables was in the range of 0.93 to 0.99, which confirmed the statistical significance of the model. Since the *p-values* were lower than 0.05, the lack of fit values were not statistically substantial. Generally, the lack of fit results varied from 0.0937 to 0.1176 for the NO_3^- and PO_4^{3-} removal, respectively, which depicted that the model was statistically significant.

3.2. Process analysis

3.2.1. COD removal

As shown in Table 4, AB, AC, BC, BD, CD, A^2, B^2, and D^2 are the significant model terms that affect the COD removal, while A, B, C, D, AD, and C^2 are excluded from the model because of their high *p-value* (≥0.05). Figure 2a shows the interaction effect of MLSS and the COD: N: P on the COD removal. The maximum COD removal (85.6%) is obtained in the lowest and highest amount of MLSS and COD: N: P (2000 mg/L and 100:8, respectively), which elucidate that the appropriate amounts of MLSS can adapt and resist the shock loading of the substrate [20]. According to Figure 2b, the maximum COD removal of 86.83% is achieved in the lowest values of MLSS and the highest aeration time (2000 mg/L and 50 min/h, respectively). These results are favorable for wastewater treatment because of the low sludge treatment process required. As shown in Table 3, the COD removal changes in the range of 78.62 % to 92.59 % except for runs 7 and 8, which illustrate the removal of 71.78 % and 57.99 %, respectively. Figure 2c depicts the interaction effects of the COD: N: P ratio and aeration time with the maximum removal of COD (89.92 %), which is observed at the aeration time of 50 min/h and the low ratio of COD: N: P (100: 4: 1). It is necessary to mention that dissolved oxygen (DO) has a considerable role in the production of extracellular polymeric substances (EPS), which can accelerate the organic material oxidation through the simulation of biomass to flocculate [19]. Hence, the flocculated microbial community can increase the trend of substrate consumption that leads to high COD removal efficiency [21]. As shown in Figure 2d, the maximum COD removal (91.32%) is detected in the highest values of COD:

Table 3. Experimental conditions and the response of SBR bioreactor.

Run	Variables				Responses					
	A: MLSS (mg/L)	B: COD:N:P	C: Aeration time (min/h)	D: Cycling time (h)	COD removal, (%)	TKN removal, (%)	PO_4^{3-} removal (%)	NO^-_3 removal (%)	SVI (mL/g)	MLVSS/MLSS
1	2000	100/4/1	40	36	81.09	80.81	48.92	65.21	65.93	0.65
2	4000	100/4/1	40	36	92.59	80.39	61.58	71.30	59.39	0.54
3	2000	100/8/2	40	36	90.73	96.42	61.38	80.12	69.65	0.57
4	4000	100/8/2	40	36	87.54	96.59	~~46.5~~	83.24	71.55	0.72
5	2000	100/4/1	50	36	90.34	91.49	60.54	60.37	68.33	0.73
6	4000	100/4/1	50	36	88.19	84.47	40.13	68.18	47.91	0.67
7	2000	100/8/2	50	36	71.78	99.13	46.81	52.31	40.36	0.72
8	4000	100/8/2	50	36	57.99	92.05	47.94	57.25	50.32	0.74
9	2000	100/4/1	40	84	92.50	80.81	59.18	62.15	54.00	0.72
10	4000	100/4/1	40	84	88.06	85.44	40.67	68.36	67.00	0.77
11	2000	100/8/2	40	84	91.44	84.94	65.50	79.84	59.00	0.68
12	4000	100/8/2	40	84	89.24	89.81	56.46	81.52	56.00	0.84
13	2000	100/4/1	50	84	89.59	75.00	44.00	71.15	77.95	0.66
14	4000	100/4/1	50	84	90.64	78.00	49.01	65.47	84.57	0.68
15	2000	100/8/2	50	84	62.23	47.00	40.00	71.10	93.79	~~1.59~~
16	4000	100/8/2	50	84	84.45	75.00	46.02	75.84	69.47	0.72
17	1000	100/6/1.5	45	60	78.62	94.58	57.84	61.17	70.70	0.67
18	5000	100/6/1.5	45	60	79.31	98.02	32.59	75.34	50.24	0.71
19	3000	100/2/0.5	45	60	79.40	54.78	25.09	66.23	46.55	0.68
20	3000	100/10/2.5	45	60	78.99	97.18	37.18	74.35	67.01	0.69
21	3000	100/6/1.5	35	60	80.86	94.41	93.13	75.11	71.53	0.74
22	3000	100/6/1.5	55	60	87.02	90.16	91.94	65.75	93.11	0.70
23	3000	100/6/1.5	45	12	88.84	97.45	77.33	67.20	72.62	0.68
24	3000	100/6/1.5	45	108	92.89	77.52	83.12	79.12	74.26	0.80
25	3000	100/6/1.5	45	60	84.13	93.72	76.26	71.12	77.80	0.69
26	3000	100/6/1.5	60	60	83.32	92.73	73.59	70.25	72.40	0.67
27	3000	100/6/1.5	60	60	86.56	93.77	73.83	70.56	71.50	0.67
28	3000	100/6/1.5	60	60	83.46	93.77	76.59	71.12	75.00	0.71
29	3000	100/6/1.5	60	60	80.13	94.46	73.22	72.15	82.00	0.71
30	3000	100/6/1.5	60	60	85.90	92.27	75.81	71.94	78.00	0.73

Table 4. ANOVA results for the process responses.

Response	Modified equations with significant terms	p-value	R^2	Adj.	SD	Mean	CV	PRESS
COD, %	Y= 83.92 – 3.44 AB – 2.89 AC – 6.68 BC +6.24 BD + 6.15 CD -1.23 A^2 – 1.17 B^2 + 1.49 D^2	<0.0001	0.97	0.94	1.86	83.93	2.21	165.27
TKN, %	Y= 93.45 + 3.27 B – 1.47 C -4.84 D – 1.16 AC +1.79 AD – 1.87 BC – 2.71 BD – 3.29 CD + 0.81 A^2 – 7.83 B^2 – 1.22 D^2	<0.0001	0.99	0.98	1.24	88.17	1.41	144.75
PO_4^{3-}, %	Y= 75.01 – 6.23 A + 2.61 B + 2.71D + 4.45 AB – 8.63 AC – 9.66 AD -6.20 BC -2.70 BD + 8.73 CD – 7.74 A^2 – 11.26 B^2 + 4.09 C^2	<0.0001	0.99	0.98	2.43	59.59	4.07	724.20
NO_3^-, %	Y= 71.19 + 3.12 A + 1.99 B – 2.97 C+ 3.43 D – 1.09 AB + 0.76 AC – 5.24 BC + 0.99 BD + 4.44 CD – 0.74 A^2 + 0.69 D^2	<0.0001	0.99	0.97	1.18	70.01	1.69	119.28
SVI, mL/g	Y= 76.02 – 5.90 A + 4.33 B + 4.36 C – 5.38 AB – 4.06 AC + 5.34 AD – 4.60 BD + 7.38 CD – 3.75 A^2 – 4.67 B^2 + 1.71 C^2	<0.0001	0.96	0.92	3.57	68.65	5.20	677.22
MLVSS/MLSS	Y= 0.70 + 0.018 A + 0.0087 B – 0.009 C + 0.024 AB + 0.013 AC + 0.044 AD – 0.029 BC – 0.031 BD – 0.034 CD	<0.0001	0.93	0.88	0.02	0.70	2.52	0.01

N: P ratio and cycling times equal to 100:8:2 and 84 h, respectively. He, et al. [22] reported the simultaneous removal of nitrogen and phosphorus by the aerobic granular SBR. The removal efficiency for NH_4^+-N, COD, and total inorganic nitrogen (TIN) was calculated as 86.53%, 95.05%, and 73.47%, respectively, in the COD: TIN ratio of 9.4 and is in agreement with the findings of the current research. The increase of cycling time in the present study caused the enhancement of COD removal efficiency. In fact, the residual COD concentration in a high cycling time could be transferred into the aerobic zone to be promptly ingested by aerobic microorganisms, which subsequently improves the COD removal efficiency [23]. Similar results were expressed by Xu et al. [24], who referred to the increase of COD removal in an expanded granular sludge blanket (EGSB) reactor as a result of MLSS enhancement. Furthermore, Desireddy and Sabumon [16] investigated the combined process of simultaneous nitrification, denitrification, and phosphorus removal in a sequencing batch airlift reactor. The removal of TN, PO_4^{3-}-P, and COD were monitored as 90.6%, 83.2%, and 90.1%, respectively. Moreover, Hayati, et al. [25] reported the overall removal efficiency of the Birjand municipal wastewater stabilization ponds as 76.16% for BOD5 and 67% for COD.

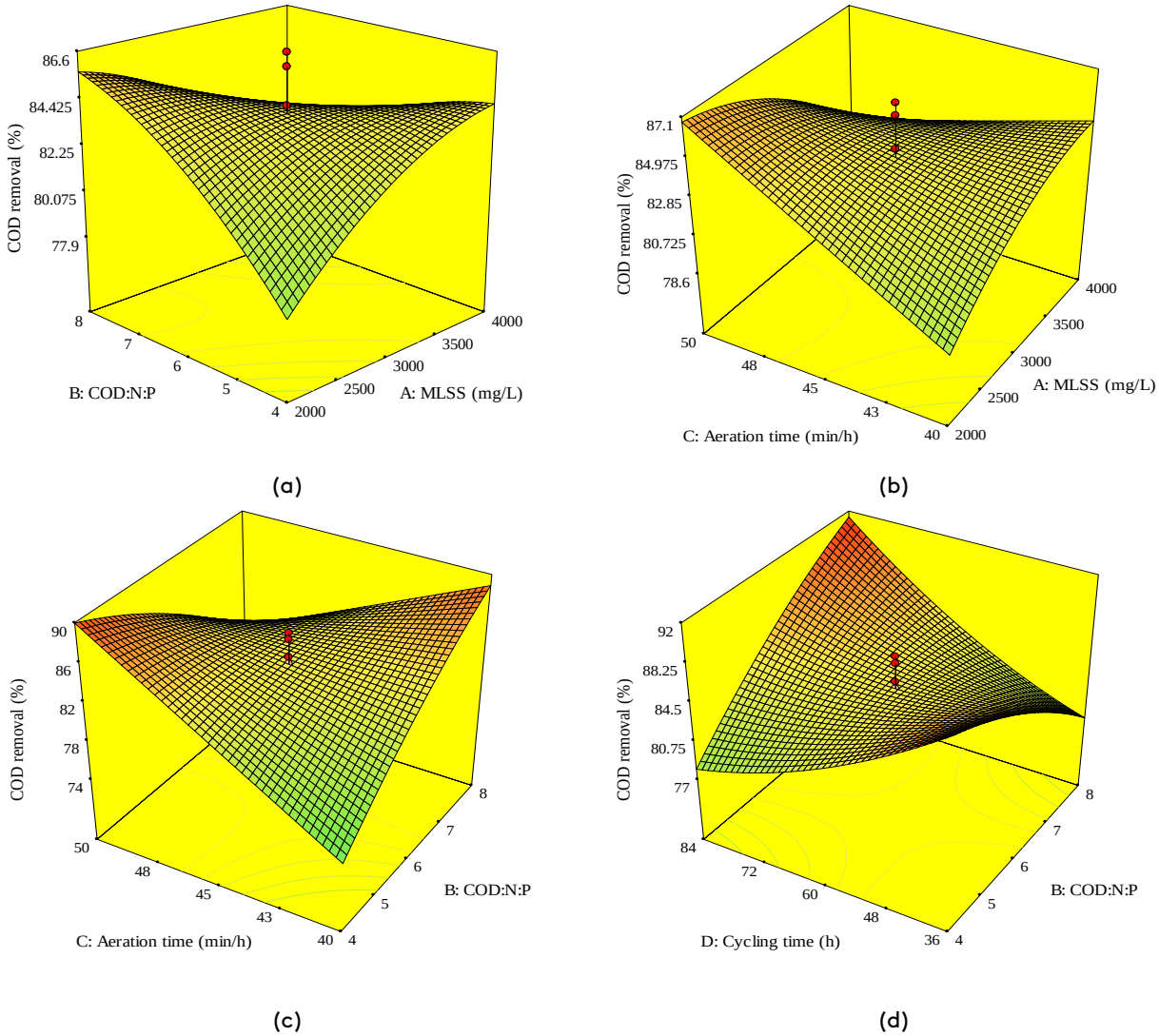

Fig. 2. The 3D plot for COD removal: (a) COD: N:P ratio and MLSS, (b) MLSS and aeration time, (c) COD: N: P ratio and aeration time, and (d) COD: N: P ratio and cycling time.

3.2.2. Total Kjeldahl nitrogen removal

According to Table 4, the significant model terms are B, C, D, AC, AD, BC, BD, CD, A^2, B^2, and D^2, while the *p-values* larger than 0.1 (A, AB, C^2) are insignificant. The interactions among the independent variables and their impacts on the ammonium removal are presented in Figure 3. The TKN removal varies between 54.78% to 99.13% and the maximum TKN removal is achieved in an MLSS concentration of 2000 mg/L, COD: N: P ratio of 100: 8: 2, aeration time of 50 min/h, and the cycling time of 36 h. It should be noted that since the nitrifiers are slow-growing bacteria, they need more aeration time to complete the nitrification process [26]. Zhang et al. [27] evaluated the capacity of the biofilm reactor for nitrogen removal from low-carbon municipal wastewater and declared the increase of nitrogen removal with the rising of aeration time. Although the low aeration time restricted the nitrification bacteria from oxidizing the ammonium concentration, a long aeration period can cause the accumulation of nitrate in the bioreactor [28]. The comparison of different plots in Figure 3 demonstrates the increase of TKN removal as a response to an increase of MLSS and reduction of the cycling time. The maximum TKN removal for AB, AC, AD, and BC is 94.86%, 96.96%, 99.35%, and 95.56%, respectively.

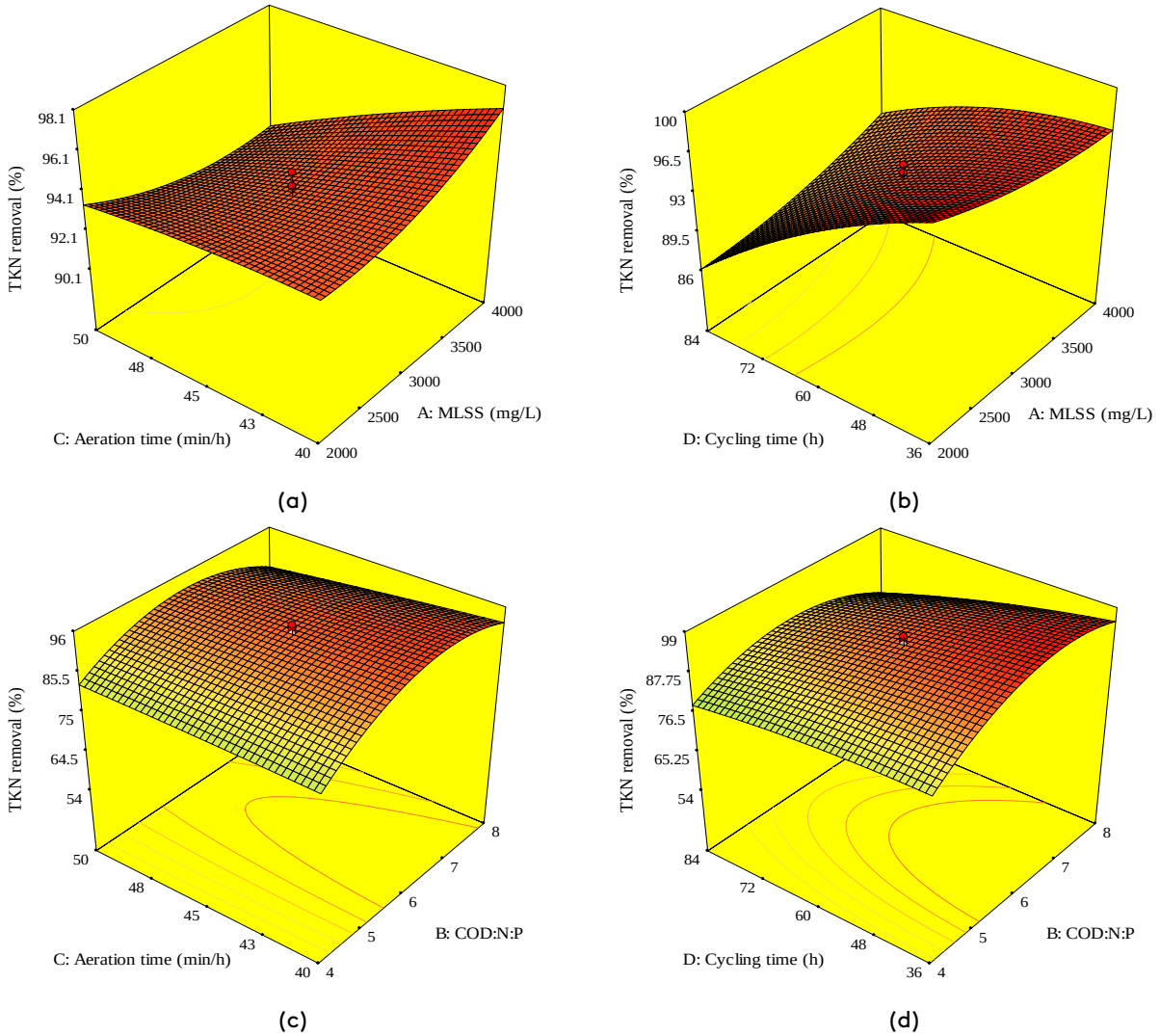

Fig. 3. The 3D plot for TKN removal: (a) MLSS and aeration time, (b) MLSS and cycling time, (c) COD: N: P ratio and aeration time, and (d) COD: N: P ratio and cycling time.

High TKN removal confirms that the nitrification and denitrification processes occur efficiently in the SBR reactor. In addition, Figure 3d illustrates that the moderate range of the COD: N: P ratio can improve the trend of ammonium removal. In fact, the amount of carbon and nitrogen in influent wastewater should be balanced to provide the energy for autotrophic nitrifiers and heterotrophic denitrifiers to remove ammonium [29,30]. Akhbari et al. [31] assessed the combined removal of carbon and nitrogen in the SBR. Their results showed the efficiency of 99% and 71% for the removal of COD and NH_4^+-N, respectively, which support the findings of 94.86% to 99.35% TKN removal in the current study.

3.2.3. Phosphorus removal

According to the ANOVA results presented in Table 4, the model terms A, B, D, AB, AC, AD, BC, BD, CD, A^2, $B^{2,}$ and C^2 are found to be significant. To simplify the model, insignificant terms such as C and D^2 are excluded from the equation. The SBR was fed with industrial wastewater containing 5, 10, 15, 20, and 25 mg/L of phosphorus concentrations. The interactions of independent parameters on the phosphorus removal are presented in Figure 4. The highest phosphorus removal was detected as 93.13% in experimental run 21 (Table 3) at an MLSS concentration of 3000 mg/L and COD: N: P ratio of 100: 6: 1.5. Therefore, the increase of influent phosphorus concentration and aeration time promoted the phosphorus accumulating organisms (PAOs) to store more phosphorus. Figure 4a illustrates the effects of MLSS concentration and COD: N: P ratio on phosphorus removal. The maximum removal of phosphorus (76.27%) is obtained at the low value of MLSS (2500 mg/L). The COD: N: P ratio at the midpoint value of 100:6:1.5 is desirable for industrial wastewater treatment. Figure 4b also depicts the collective effects of MLSS concentration and the cycling time on the removal percentage of phosphorus. The maximum phosphorus removal was 87.18% in the low value of MLSS and the highest cycling times of 2000 mg/L and 84 h, respectively. According to the obtained results, the low amount of MLSS in the bioreactor is very significant because the sludge bulking and SVI enhancement occur as a result of a high amount of MLSS [32]. The effect of MLSS in the performance of the modified A_2O process was investigated by Fan et al. [20]. Their results demonstrated that the increase of MLSS to 2000 mg/L led to total phosphorus (TP) removal, while it was depleted at the MLSS of 2000-4000 mg/L, which confirmed the output of this study. Another literature [33] reported the decline of 80% phosphorus removal efficiency and 37% phosphorus release as a result of the MLSS increment.

Figure 4c shows the interaction of COD: N: P ratio and aeration time on phosphorus removal. The highest phosphorus removal is observed at the COD: N: P ratio of 100: 6: 1.5 and the lowest aeration time of 40 min/h to achieve 81.03 % of the phosphorus removal. Moreover, Figure 4d displays the maximum percentage of phosphorus removal equal to 91.44%, which is observed in the highest value of aeration time and cycling time as 50 min/h and 84 h, respectively. The midpoint value of the COD: N: P ratio in all the experiments is found to be the most suitable condition to achieve the maximum removal of nutrients. It can be speculated that the high C: N ratio fluctuates the distribution of substrates and microbial communities by increasing glycogen accumulating organisms (GAOs) and PAOs competition, which the dominance of GAOs finally occurs. Hence, the higher COD: N ratio causes the excessive growth of GAOs and reduction of phosphorus removal [34]. Overall, the phosphorus removal changes in the range of 25.09% to 93.13%.

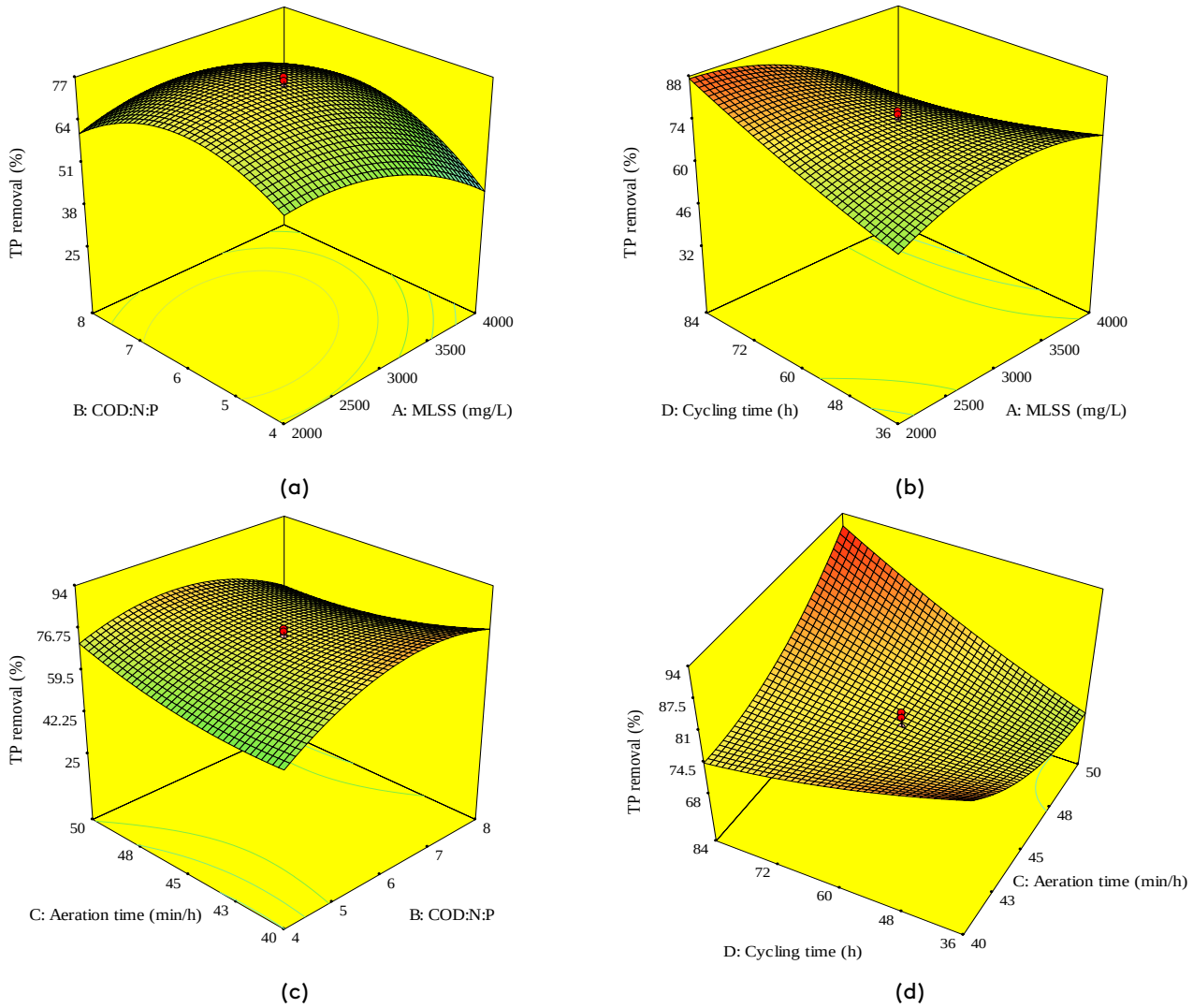

Fig. 4. The 3D plot for phosphorus removal: (a) MLSS and COD: N: P ratio, (b) MLSS and cycling time, (c) COD: N: P ratio and aeration time, and (d) aeration time and cycling time.

3.2.4. Nitrate removal

The ANOVA results for NO_3^- removal are presented in Table 4. The following are significant model terms: variables A, B, C, and D; the interactive terms AB, AC, BC, BD, and CD; and the second-order effects of A^2, D^2. The insignificant model terms of AD, B^2, and C^2 are excluded. The interaction effects of the variables on the NO_3^- removal are illustrated in Figure 5. The maximum NO_3^- removal (83.24%) is obtained when the MLSS concentration value is set at 4000 mg/L, COD: N: P ratio of 100: 8: 2 at an aeration time of 40 min/h, and cycling duration of 36 h. The NO_3^- removal varies between 52.31% to 83.24% depending on the experimental conditions. Sayadi, et al. [35] recorded the highest NO_3^- removal in the range of 81.49-89.8% on the eighth day of the experiment. According to Figures. 5a and 5b, the enhancement of MLSS concentration (4000 mg/L) cause an increase in the NO_3^- removal efficiency. Moreover, Figures. 5a and 5d show that the highest NO_3^- removal efficiency is achieved while the COD: N: P ratio is set at 100: 8: 2, demonstrating that the rich carbon source leads to a higher denitrification performance and lower nitrogen content in the effluent. Generally, the rate of denitrification process attributes to the type of carbon source, substrate bioavailability and biodegradability, and COD: TN ratio [36]. However, the insufficient supply of organic carbon in the low COD: TN ratio leads to incomplete denitrification, which Ge et al. [37] expressed in their study of the anoxic denitrification process under various COD: N ratios. The increase of the COD: N ratio from 1 to 25

developed the denitrification rate and accelerated the trend of nitrate removal, which was consistent with the obtained results in the present study. The maximum NO_3^- removals in the combined effects of AB, AC, BC, and BD were 74.22%, 75.56%, 80.95%, and 78.05%, respectively. The optimum conditions for the aeration and cycling times were 50 min/h and 84 h, respectively, as given in Figures. 5b-d. Although the negative impact of the high aeration time on nitrate removal was completely obvious, the present study demonstrated that the aeration time of 50 min/h was the optimum value to obtain the high nitrate removal, which was in accordance with He et al. [28] who reported the reliable nitrogen removal performance in the high aeration time.

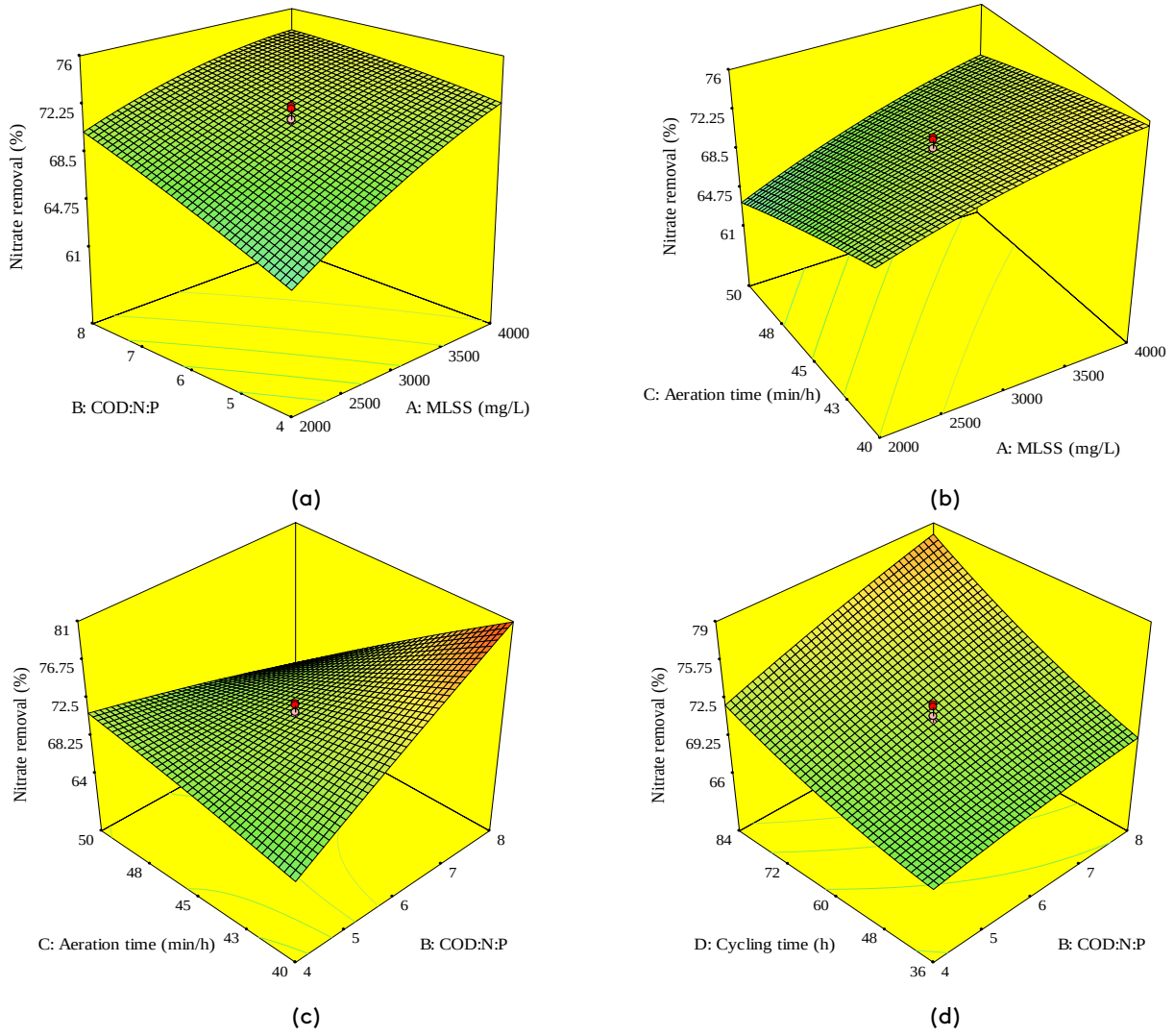

Fig. 5. The 3D plot for nitrate removal: (a) MLSS and COD: N: P ratio, (b) MLSS and aeration time, (c) COD: N: P ratio and aeration time, and (d) COD: N: P ratio and cycling time.

3.2.5. Sludge volume index

The interaction effects of all the variables on SVI were significant except for the effect of D and D^2. The SVI results varied between 46.55 mL/g to 93.79 mL/g in all the experiments (Figure 6). The maximum and minimum SVI values in the experimental runs were15 and 19, respectively. Regarding the obtained results, the high value of nitrogen in the wastewater was an effective parameter on the granule formation that caused the activated sludge to be deformed and expand in the bioreactor. In reverse, the activated sludge was

compacted, and the settlement speed improved in the low nitrogen concentration. Based on Figure 6a, the high value of MLSS is desirable to get 60.93 mL/g of SVI, which is in agreement with Akhbari et al. [31], who reported the minimum SVI value as 71.69 mL/g when the MLSS concentration and HRT were 10000 mg/L and 6 h, respectively. Furthermore, the lower SVI is achieved while there is a rise in the MLSS concentration and a decline in the cycling time. The low SVI in Figure 6b is observed in the highest MLSS concentration and the moderate aeration time of 4000 mg/L and 45 min/h, respectively. It is noteworthy to mention that the low aeration time can upgrade the growth rate and settle ability of biomass such as heterotrophs and filamentous bacteria. In other words, the reduction of aeration time mitigates the hydraulic shear force that leads to easily and rapidly sludge settling [28,38]. Azizi et al. [39] demonstrated that a low rate of aeration (30 L/h) was effective enough to reach a high removal in an SBR bioreactor. These results were similar to the observed results in the current study, showing a low aeration rate to be more suitable for industrial wastewater treatment. In addition, the optimum cycling time for decreasing the SVI was 36 h (Figures. 6c and 6d). Overall, the SVI values for AB, AC, AD, and BD were 60.93, 66.39, 60.24, and 61.58 mL/g, respectively.

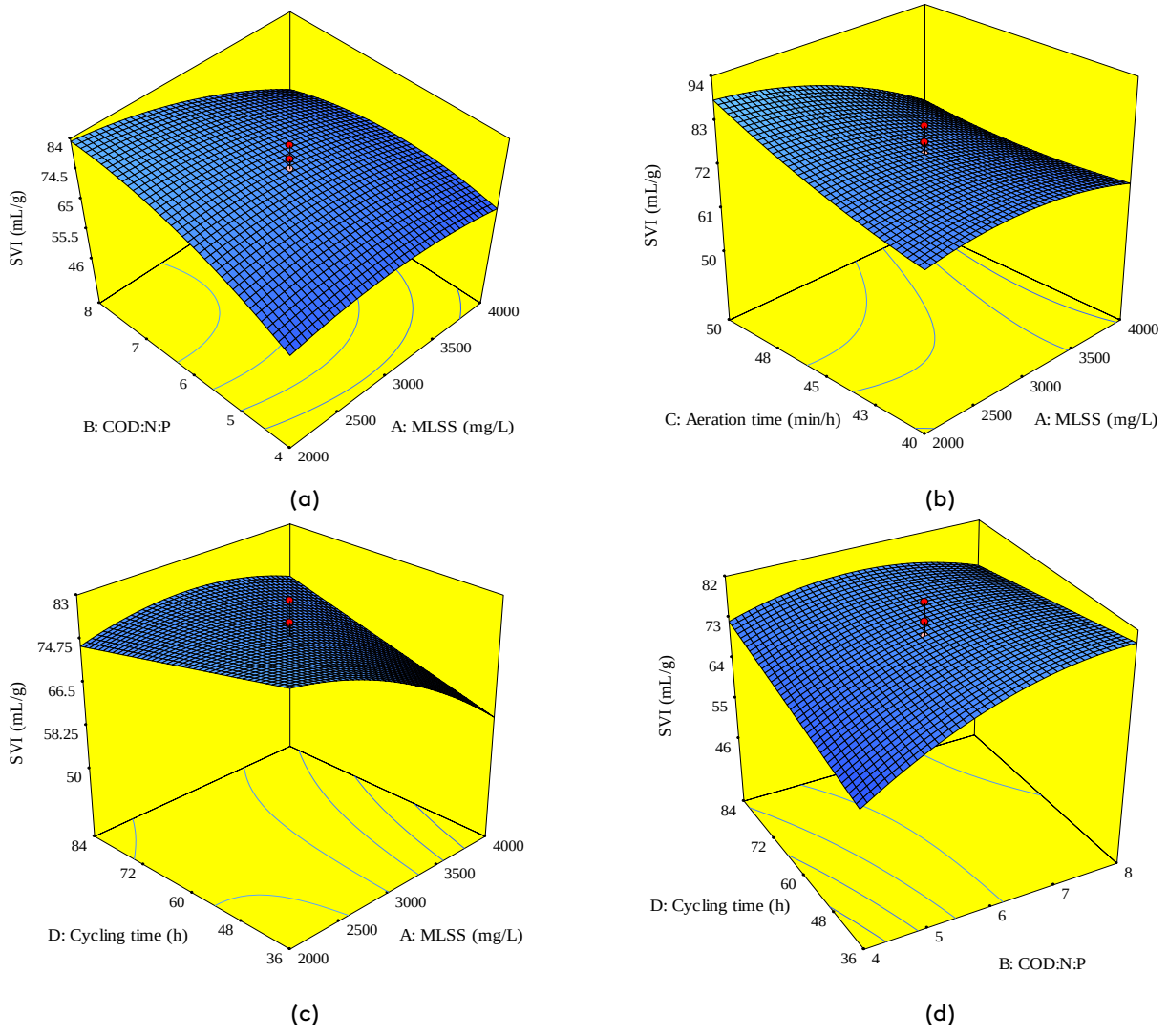

Fig. 6. The 3D plot for SVI: (a) MLSS and COD: N:P ratio, (b) MLSS and aeration time, (c) MLSS and cycling time, and (d) COD: N: P ratio and cycling time.

3.2.6. The amount of MLVSS/MLSS

According to Table 4, the significant model terms were A, B, C, AB, AC, AD, BC, BD, and CD. Figure 7 depicts the interaction effects of four independent variables on the MLVSS/MLSS ratio under the batch condition. The maximum and minimum concentrations of the MLVSS/MLSS ratio are observed in the experimental runs 12 and 2, respectively. The independent variables of MLSS and the COD: N: P ratio had significant impacts on the MLVSS/MLSS ratio. The 4000 mg/L of MLSS concentration was appropriate to improve the MLVSS/MLSS ratio in the wastewater treatment system, which was attributed to the higher concentration of microorganisms present in the aeration tank. Furthermore, the impacts of the aeration time and the highest cycling time on the MLVSS/MLSS ratio were unavoidable. In fact, the long-term operation in the reactor may accumulate the biomass content and subsequently increase the ratio of MLVSS/MLSS [28].

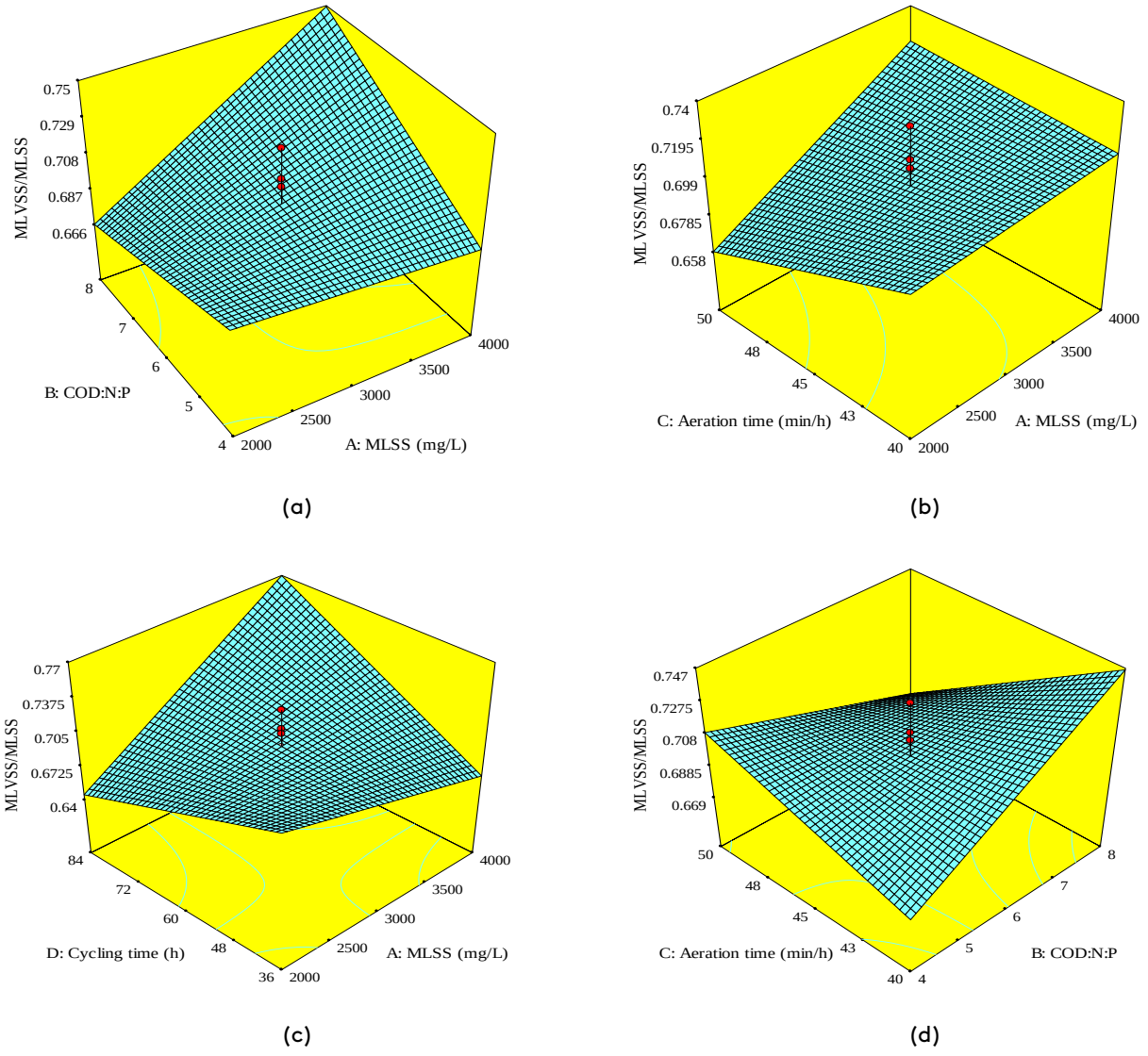

Fig. 7. The 3D plot for MLVSS/MLSS ratio: (a) MLSS and COD: N: P ratio, (b) MLSS and aeration time, (c) MLSS and cycling time, and (d) COD: N: P ratio and aeration time.

Additionally, the increase of operational time may decrease the rate of MLSS production, which eventually leads to the diminution of the MLVSS/MLSS ratio. The average value of the MLVSS/MLSS ratio was higher than that of Fan et al. [40] that was in the range of 0.216 to 0.411, which illustrated higher activated sludge activity. However, the MLVSS/MLSS ratio reveals the activity of activated sludge that depends on the sludge age, influent COD, and contact time. It should be mentioned that the MLVSS/MLSS value is usually 0.75 in municipal wastewater [41], which is approximately similar to the present study.

3.3. Optimization of operational conditions

The optimum condition was obtained according to the variables (MLSS, COD: N: P, cycling time, and aeration time) and responses (COD%, TKN%, NO_3^-%, PO_4^{3-}%, SVI, and MLVSS/MLSS). Four points within the optimal ranges were chosen, and the precision of the models was evaluated in the batch system. Then, the actual data were compared with the corresponding predicted values. The *p-value* close to one was determined under numerical optimization. The results of four experiments in the optimum region are shown in Table 5. In the first run, the highest *p-values* (0.840) are detected in the MLSS of 4000 mg/L, COD: N: P ratio of 100: 8, aeration time of 40 min/h, and cycling time of 40 h. Moreover, the empirical data is in close agreement with the predicted ones.

3.4. Quantification of nitrification and denitrification rate

The nitrification rate (N_r) determines the fate of ammonium, and subsequently, the time period needed for nitrogen removal [42]. The calculation of N_r is illustrated in Equation (2):

$$N_r = \frac{NH_4^+ - N_i - NH_4^+ - N_f}{HRT} \quad (2)$$

where NH_4^+-N_i and NH_4^+-N_f are the initial and final ammonium concentrations, respectively. The variation of TKN removal in the SBR reactor is illustrated in Figure 8a.

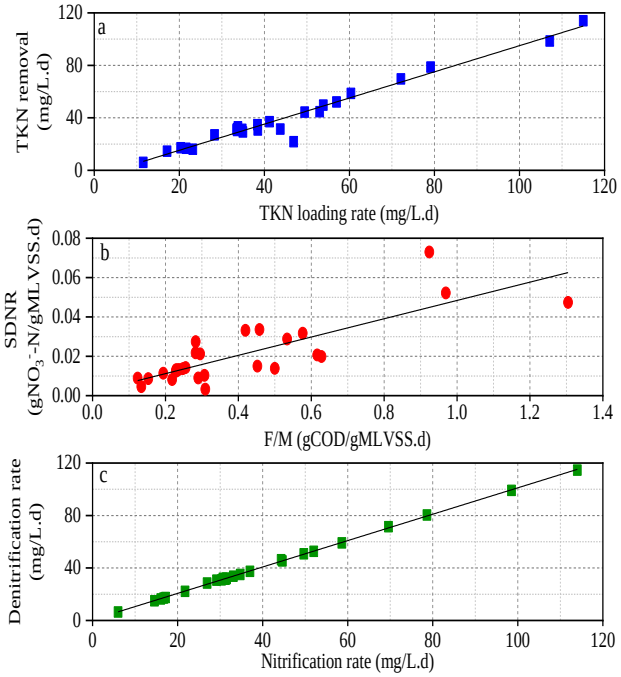

Fig. 8. The trend of TKN removal in various TKN concentrations (a), the impact of F/M ratio on SDNR at steady state (b), and variation of nitrification and denitrification rates (c).

Table 5. Considered criteria for optimum conditions.

				Predicted values						Experimental values					
MLSS, mg/L	COD:N:P	Aeration time, min/h	Cycling time, h	COD	TKN	PO_4^{3-}	NO_3^-	SVI	MLVSS/MLSS	COD	TKN	PO_4^{3-}	NO_3^-	SVI	MLVSS/MLSS
4000	100:8:2	40	40	87.1	95.5	93.1	81.9	67.09	0.73	82.5	89.8	87.2	73.5	64.8	0.8
4000	100:6:1.5	40	36	90.8	95.9	91.5	70.3	69.07	0.63	87.4	91.5	85.6	69.7	55.9	0.8
3500	100:4:1	50	48	88.1	87.9	61.1	69.0	65.78	0.70	83. 5	84.2	57.4	62.4	63.5	0.7
2600	100:8:2	40	84	91.0	85.3	69.4	80.8	62.49	0.73	86.8	80.3	65.3	77.1	59.1	0.8

As shown in Figure 8a, the TKN removal is enhanced significantly while the TKN loading rate increases from 11.53 mg/L.d to 114.99 mg/L.d. However, a significant reduction in the trend of TKN removal is observed when the cycling time is upgraded from 1.5 d to 3.5 d. Regarding the TKN loading rate of

46.89 mg/L.d with a cycling time of 3.5 d, the TKN removal decreases to 21.75 mg/L.d, which is 41.67% lower than the same condition at a 1.5 d cycling time. Generally, the carbon and nutrient removal efficiencies in the SBR systems depend directly on the duration of the cycling time and time needed for each phase of the process. Although the increase of cycle time promotes the nutrient removal efficiency, the high influent flow finally results in the enhancement of the final cost. Therefore, the optimal condition of a system should be considered simultaneously from the pollutant removal and economic point of view [43]. The determination of the denitrification rate (D_r) is based on the consumption of nitrate by denitrifiers as shown in Equation (3).

$$D_r = \frac{NO_3^- - N_i - NO_3^- - N_f}{HRT} \quad (3)$$

where NO_3^--N_i and NO_3^--N_f are the initial and final nitrate concentrations in the bioreactor, respectively. Furthermore, the specific denitrification rate (SDNR) is measured using Equation (4):

$$SDNR = \frac{Q \times \Delta NO_3^- - N}{V \times MLVSS} \quad (4)$$

where Q is the flow rate (L/d) and Δ NO_3^--N is the nitrate removal (mg/L). Also, *V* and *MLVSS* are the bioreactor volume (L) and biomass concentration (mg/L), respectively. The impact of the F/M ratio on SDNR is plotted in Figure 8b and depicts the development of SDNR coinciding with the F/M ratio progress. The maximum ratio of SDNR was detected for the F/M ratio of 0.92 mg COD/mg MLVSS.d, while an increase in the F/M ratio at 1.3 mg COD/mg MLVSS. d caused a minimum SDNR of 0.05 mgNO_3^--N/mg MLVSS.d, explained by the adverse effect of a high organic loading rate, which caused the endogenous decay among the active biomass and eventually led to NO_x release.The considerable alterations of SDNR were observed at the adjusted range of COD: TN ratios. Although the negative effect of a high COD: TN ratio on SDNR is obvious because of free nitrous acid (FNA) inhibition [44,45], the increase of the COD: TN ratio in the present study from 100:4 to 100:8 caused 7-fold progress in the amount of SDNR in run 7. The more available nitrogen source led to the high denitrification rate. Corresponding to runs 14 and 17, the SDNR dramatically increased from 0.009 to 0.052 mgNO_3^--N/mgMLVSS.d, while the COD: TN ratio reached 100:6. Similar results were reported by Badia et al. [36]; they investigated the impact of the SCOD: N ratio on SDNR in the SBR bioreactor and declared the linear increase of SDNR with an increment of SCOD: N ratio in the range of 3-6.6. The nitrification and denitrification rates differed significantly (p<0.05) in the various operational runs. As can be seen in Figure 8c, the nitrification rate is enhanced along with the denitrification rate. Since the DO concentration was kept constant at 2 mg/L, the reduction of the nitrification rate in some operational runs was not as result of the low DO, but it can be due to the multiple cycling times. The increase in cycling time from 1.5 to 3.5 d led to the decrease of the nitrification rate to 21.7 mg/L.d, with the influent TKN concentration of 164 mg/L. Since the optimum cycling time for the SBR function was determined to be approximately 1.5 d, the higher cycling time might inhibit the activity of nitrifying biomass. On the other hand, doubling the TKN concentration to 172.5 mg/L with a cycling time of 1.5 d resulted in a triple-increase in the nitrification rate (113.9 mg/L.d) despite the relatively low MLVSS concentration. A positive tendency was observed between the nitrification rate and COD: TN ratio as a fundamental parameter. The peak of the nitrification rate was detected at the COD: TN ratio of 100: 8, which optimized the operational condition for ammonium oxidizing bacteria (AOB) and nitrite-oxidizing bacteria (NOB). The relatively sensible fluctuations occurred at a COD: TN ratio lower than 100: 6, which could be associated with the severe competition between heterotrophs and nitrifiers for the COD uptake that limits the proliferation of AOB and NOB [46]. In addition, the lower COD: TN ratio probably caused the consequent increase of partial nitrification and nitrite accumulation [2]. A high denitrification rate is acquired when nitrite or nitrate is used as an electron acceptor and organic matter as an electron donor to reduce nitrate [44]. In addition, the rate of denitrification mostly depends on the type of carbon source and its degradability and COD: NO_3^--N ratio [37]. Hence, the largest denitrification rate (114.5 mg/L.d) was measured when the initial nitrate concentration reached 172.6 mg/L (Figure 8c). Nevertheless, the

denitrification rate drastically dropped to 20 mg/L.d in the initial nitrate concentration range of 52.8-61.9 mg/L due to the long adjusted cycling time. Similarly, Ge et al. [37] reported the lowest specific nitrate reduction rate at 4-8 h, which upgraded to 0.029 d at 2-4 h, where the maximum specific carbon consumption rate was detected. Furthermore, the effect of the COD: NO_3^--N ratio on the whole denitrification process is not negligible so that the low ratio of COD: NO_3^--N equal to 100: 1 led to the minimum denitrification ratio (6.5 mg/L.d), owing to insufficient organic matters. As the COD: NO_3^--N ratio was modified as low as 8, the denitrification rate maximized, which was in line with the findings of Ge et al. [37]; they discovered the positive relationship between the high COD: NO_3^--N ratio and nitrite accumulation that finally caused the incomplete denitrification. In other words, the removal of excess nitrate concentration in the anoxic tank requires more available COD to maintain and stimulate the biomass. Therefore, the lack of COD may disrupt the denitrification phenomenon and accumulate other intermediates.

4. Conclusions

Highly efficient simultaneous CNP removal was successfully achieved in the SBR. The maximum removals for COD, TKN, PO_4^{3-}, NO_3^- and the amounts of SVI and MLVSS/MLSS were 92.59%, 99.13%, 93.13%, 83.24%,46.55 mL/g, and 0.84, respectively. The optimum condition of the SBR reactor to treat industrial wastewater was achieved at an MLSS concentration of 4000 mg/L, COD: N: P of 100: 8: 2, the aeration flow rate of 40 min/h, and 40 h of cycling time. Furthermore, the results demonstrated that the SDNR strictly relied on the F/M ratio; the nitrification rate depended on the influent ammonium concentration and COD: TN ratio. The results of the present study could expose new scenarios for industrial wastewater treatment in further investigations.

Acknowledgment

This research was carried out with the financial support of the Islamic Azad University, Tonekabon Branch, Iran.

References

[1] Amini, M., Khoei, Z. A., Erfanifar, E. (2019). Nitrate (NO_3^-) and phosphate (PO_4^{3-}) removal from aqueous solutions by microalgae Dunaliella salina. *Biocatalysis and agricultural biotechnology, 19*, 101097.

[2] Moradi, S., Zinatizadeh, A., Zinadini, S., Gholami, F. (2021). High-rate CNP removal from wastewater in a single jet loop air lift bioreactor: Process modeling and optimization with four process and operating factors. *Journal of water process engineering*, *40*, 101980.

[3] Nguyen, T. T., Némery, J., Gratiot, N., Strady, E., Tran, V. Q., Nguyen, A. T., Aimé, J., Peyne, A. (2019). Nutrient dynamics and eutrophication assessment in the tropical river system of Saigon–Dongnai (southern Vietnam). *Science of the total environment*, *653*, 370-383.

[4] Watsuntorn, W., Ruangchainikom, C., Rene, E. R., Lens, P. N., Chulalaksananukul, W. (2019). Comparison of sulphide and nitrate removal from synthetic wastewater by pure and mixed cultures of nitrate-reducing, sulphide-oxidizing bacteria. *Bioresource technology*, *272*, 40-47.

[5] Crini, G., Lichtfouse, E. (2019). Advantages and disadvantages of techniques used for wastewater treatment. *Environmental chemistry letters*, *17*(1), 145-155.

[6] Fayazi, M. (2020). Removal of mercury (II) from wastewater using a new and effective composite: sulfur-coated magnetic carbon nanotubes. *Environmental science and pollution research, 27*(11), 12270-12279.

[7] Fayazi, M., Ghanbarian, M. One-pot hydrothermal synthesis of polyethylenimine functionalized magnetic clay for efficient removal of noxious Cr (VI) from aqueous solutions. *Silicon, 12*(1), 125-134.

[8] Khaki, E., Abyar, H., Nowrouzi, M., Younesi, H., Abdollahi, M., Enderati, M. G. (2021). Comparative life cycle assessment of polymeric membranes: Polyacrylonitrile, polyvinylimidazole and poly (acrylonitrile-co-vinylimidazole) applied for CO_2 sequestration. *Environmental technology and innovation*, *22*, 101507.

[9] Abyar, H., Younesi, H., Bahramifar, N., Zinatizadeh, A. A. (2018). Biological CNP removal from meat-processing wastewater in an innovative high rate up-flow A_2O bioreactor. *Chemosphere, 213,* 197-204.

[10] Li, J., Wu, B., Li, Q., Zou, Y., Cheng, Z., Sun, X., Xi, B. (2019). Ex situ simultaneous nitrification-denitrification and in situ denitrification process for the treatment of landfill leachates. *Waste management, 88,* 301-308.

[11] Lei, X., Jia, Y., Chen, Y., Hu, Y. (2019). Simultaneous nitrification and denitrification without nitrite accumulation by a novel isolated *Ochrobactrum anthropic* LJ81. *Bioresource technology, 272,* 442-450.

[12] Iorhemen, O. T., Hamza, R. A., Zaghloul, M. S., Tay, J. H. (2019). Aerobic granular sludge membrane bioreactor (AGMBR): Extracellular polymeric substances (EPS) analysis. *Water research, 156,* 305-314.

[13] Lotti, T., Carretti, E., Berti, D., Martina, M. R., Lubello, C., Malpei, F. (2019). Extraction, recovery and characterization of structural extracellular polymeric substances from anammox granular sludge. *Journal of environmental management, 236,* 649-656.

[14] Soler-Jofra, A., Wang, R., Kleerebezem, R., van Loosdrecht, M. C., Pérez, J. (2019). Stratification of nitrifier guilds in granular sludge in relation to nitritation. *Water research, 148,* 479-491.

[15] Cerruti, M., Stevens, B., Ebrahimi, S., Alloul, A., Vlaeminck, S. E., Weissbrodt, D. G. (2020). Enrichment and aggregation of purple non-sulfur bacteria in a mixed-culture sequencing-batch photobioreactor for biological nutrient removal from wastewater. *Frontiers in bioengineering and biotechnology, 8,* 557234. doi: 10.3389/fbioe.2020.557234.

[16] Desireddy, S., Sabumon, P. (2021). Development of aerobic granulation system for simultaneous removal of C, N, and P in sequencing batch airlift reactor. *Journal of Environmental chemical engineering, 9*(5), 106100.

[17] Fayazi, M., Afzali, D., Taher, M., Mostafavi, A., Gupta, V. (2015). Removal of Safranin dye from aqueous solution using magnetic mesoporous clay: Optimization study. *Journal of molecular lquids, 212,* 675-685.

[18] Nowrouzi, M., Abyar, H. (2021). A framework for the design and optimization of integrated fixed-film activated sludge-membrane bioreactor configuration by focusing on cost-coupled life cycle assessment. *Journal of cleaner production, 296,* 126557.

[19] APHA, 1999. Standard methods for the examination of water and wastewater, American public health association, Washington, DC.

[20] Fan, J., Ye, J., Zhang, H., Ji, B., Ye, W. (2018). Integrated Effect of MLSS and SRT on Performance of a full-scale modified A^2/O Process. *Polish journal of environmental studies, 27*(4), 1475-1482

[21] Hauduc, H., Al-Omari, A., Wett, B., Jimenez, J., De Clippeleir, H., Rahman, A., Wadhawan, T., Takacs, I. (2019). Colloids, flocculation and carbon capture–a comprehensive plant-wide model. *Water science and technology, 79*(1), 15-25.

[22] He, Q., Zhang, S., Zou, Z., Zheng, L., Wang, H. (2016). Unraveling characteristics of simultaneous nitrification, denitrification and phosphorus removal (SNDPR) in an aerobic granular sequencing batch reactor. *Bioresource technology, 220,* 651-655.

[23] Amini, M., Younesi, H., Najafpour, G., Zinatizadeh-Lorestani, A. A. (2012). Application of response surface methodology for simultaneous carbon and nitrogen (SND) removal from dairy wastewater in batch systems. *International journal of environmental studies, 69*(6), 962-986,

[24] Xu, H., Liu, Y., Gao, Y., Li, F., Yang, B., Wang, M., Ma, C., Tian, Q., Song, X., Sand, W. (2018). Granulation process in an expanded granular sludge blanket (EGSB) reactor for domestic sewage treatment: Impact of extracellular polymeric substances compositions and evolution of microbial population. *Bioresource technology, 269,* 153-161.

[25] Hayati, H., Doosti, M., Sayadi, M. (2013). Performance evaluation of waste stabilization pond in Birjand, Iran for the treatment of municipal sewage. *Proceedings of the*

international academy of ecology and environmental sciences, 3(1), 52-58.

[26] He, Q., Zhang, W., Zhang, S., Wang, H. (2017). Enhanced nitrogen removal in an aerobic granular sequencing batch reactor performing simultaneous nitrification, endogenous denitrification and phosphorus removal with low superficial gas velocity. *Chemical engineering journal, 326,* 1223-1231.

[27] Zhang, L., Huang, Y., Li, S., He, P., Wang, D. (2018). Optimization of nitrogen removal in solid carbon source SND for treatment of low-carbon municipal wastewater with RSM method. *Water, 10*(7), 827. doi:10.3390/w10070827.

[28] He, Q., Chen, L., Zhang, S., Wang, L., Liang, J., Xia, W., Wang, H., Zhou, J. (2018). Simultaneous nitrification, denitrification and phosphorus removal in aerobic granular sequencing batch reactors with high aeration intensity: Impact of aeration time. *Bioresource technology, 263,* 214-222.

[29] Li, J., Meng, J., Li, J., Wang, C., Deng, K., Sun, K., Buelna, G. (2016). The effect and biological mechanism of COD/TN ratio on nitrogen removal in a novel upflow microaerobic sludge reactor treating manure-free piggery wastewater. *Bioresource technology, 209,* 360-368.

[30] Mannina, G., Capodici, M., Cosenza, A., Di Trapani, D., van Loosdrecht, M. C. (2017). Nitrous oxide emission in a University of Cape Town membrane bioreactor: the effect of carbon to nitrogen ratio. *Journal of cleaner production, 149,* 180-190.

[31] Akhbari, A., Zinatizadeh, A., Mohammadi, P., Irandoust, M., Mansouri, Y. (2011). Process modeling and analysis of biological nutrients removal in an integrated RBC-AS system using response surface methodology. *Chemical engineering journal, 168*(1), 269-279.

[32] Zou, J., Pan, J., Wu, S., Qian, M., He, Z., Wang, B., Li, J. (2019). Rapid control of activated sludge bulking and simultaneous acceleration of aerobic granulation by adding intact aerobic granular sludge. *Science of the total environment, 674,* 105-113.

[33] Salehi, S., Cheng, K. Y., Heitz, A., Ginige, M. P. (2019). A novel storage driven granular post denitrification process: Long-term effects of volume reduction on phosphate recovery. *Chemical engineering journal, 356,* 534-542.

[34] Onetto, C. A., Eales, K. L., Guagliardo, P., Kilburn, M. R., Gambetta, J. M., Grbin, P. R. (2017). Managing the excessive proliferation of glycogen accumulating organisms in industrial activated sludge by nitrogen supplementation: A FISH-NanoSIMS approach. *Systematic and applied microbiology, 40,* 500-507.

[35] Sayadi, M., Ahmadpour, N., Fallahi, C. M., Rezaei, M. (2016). Removal of nitrate and phosphate from aqueous solutions by microalgae: An experimental study. *Global Journal of environmental science and management, 2*(4), 357-364.

[36] Badia, A., Kim, M., Nakhla, G., Ray, M. B. (2019). Effect of COD/N ratio on denitrification from nitrite. *Water environment research, 91*(2), 119-131

[37] Ge, S., Peng, Y., Wang, S., Lu, C., Cao, X., Zhu, Y. (2012). Nitrite accumulation under constant temperature in anoxic denitrification process: The effects of carbon sources and COD/NO_3-N. *Bioresource technology, 114,* 137-143.

[38] Vjayan, T., Vadivelu, V. (2017). Effect of famine-phase reduced aeration on polyhydroxyalkanoate accumulation in aerobic granules. *Bioresource technology, 245,* 970-976.

[39] Aziz, S. Q., Aziz, H. A., Yusoff, M. S., Bashir, M. J. (2011). Landfill leachate treatment using powdered activated carbon augmented sequencing batch reactor (SBR) process: Optimization by response surface methodology. *Journal of hazardous materials, 189*(1-2), 404-413.

[40] Fan, J., Ji, F., Xu, X., Wang, Y., Yan, D., Xu, X., Chen, Q., Xiong, J., He, Q. (2015). Prediction of the effect of fine grit on the MLVSS/MLSS ratio of activated sludge. *Bioresource technology, 190,* 51-56.

[41] Zhang, J., Shao, Y., Wang, H., Liu, G., Qi, L., Xu, X., Liu, S. (2021). Current operation state of wastewater treatment plants in urban China. *Environmental research, 195,* 110843.

[42] Kraus, T. E., O'Donnell, K., Downing, B. D., Burau, J. R., Bergamaschi, B. (2017). Using paired in situ high frequency nitrate

measurements to better understand controls on nitrate concentrations and estimate nitrification rates in a wastewater-impacted river. *Water resources research, 53*(10), 8423-8442.

[43] Debik, E., Manav, N. (2010). Sequence optimization in a sequencing batch reactor for biological nutrient removal from domestic wastewater. *Bioprocess and biosystems engineering, 33*(5), 533-540.

[44] Ribera-Guardia, A., Marques, R., Arangio, C., Carvalheira, M., Oehmen, A., Pijuan, M. (2016). Distinctive denitrifying capabilities lead to differences in N_2O production by denitrifying polyphosphate accumulating organisms and denitrifying glycogen accumulating organisms. *Bioresource technology, 219,* 106-113.

[45] Wang, S., Deng, L., Zheng, D., Wang, L., Zhang, Y., Yang, H., Jiang, Y., Huang, F. (2018). Control of partial nitrification using pulse aeration for treating digested effluent of swine wastewater. *Bioresource technology, 262,* 271-277.

[46] Ge, S., Wang, S., Yang, X., Qiu, S., Li, B., Peng, Y. (2015). Detection of nitrifiers and evaluation of partial nitrification for wastewater treatment: a review. *Chemosphere, 140,* 85-98.